Adaptive Learning for Controlled Lagrangian Particle Tracking

Sungjin Cho*, Fumin Zhang*, Catherine R. Edwards†
*School of Electrical and Computer Engineering
Georgia Institute of Technology, Atlanta, Georgia 30308
Email: scho88, fumin@gatech.edu
†Skidaway Institute of Oceanography, University of Georgia, Savannah, Georgia, 31411
Email: catherine.edwards@skio.uga.edu

***Abstract*—Controlled Lagrangian particle tracking (CLPT) is a feedback control methodology for autonomous underwater vehicles (AUVs) in dynamic ocean environments that can reveal information about ocean flow and model error through the operation of AUVs. From CLPT, we evaluate the navigational performance of AUVs with controlled Lagrangian prediction error (CLPE), which represents the difference between the predicted and true trajectories of AUVs. In this paper, using CLPE, we develop an adaptive learning algorithm that allows AUVs to learn their true motion in ocean flow fields in real time. While previous work shows that CLPE increases over time in simulated and field experiments, the proposed algorithm forces CLPE to converge to zero so that the vehicle motion model is unique and flow fields can be identified. For the robustness of the proposed algorithm, we prove that CLPE is ultimately bounded under disturbances. The proposed algorithm is verified by simulation results.**

I. Introduction

Over the past decades, autonomous underwater vehicles (AUVs) have proven to be valuable sensing platforms in a variety of scientific and practical missions [1]: oil spill survey [2], acoustic mapping [3], and ocean sampling [4], among many others. High navigational performance of AUVs is essential for persistent and efficient collection of information-rich data [5], and serious performance degradation can result when flow speed is comparable to or exceeds AUV forward speed, as is the case for underwater gliders [6], [7].

Controlled Lagrangian particle tracking (CLPT) is a feedback control methodology for AUVs moving in dynamic ocean environments [8], [9] that has been demonstrated to reveal information about the flow field through which the vehicles move. In contrast to *passive* Lagrangian methods, an AUV is viewed as a *controlled* Lagrangian particle in the sense that AUVs are not freely advected by ocean flow. To track the controlled Lagrangian particle, we generate the predicted trajectory of the AUV by simulating vehicle motion models composed of incorporated flow models and controllers. Then, we compare the predicted trajectory with the measured true trajectory of the AUV. The discrepancy between the two trajectories shows the tracking performance of the controlled Lagrangian particle, called controlled Lagrangian prediction error (CLPE). CLPE is a crucial measure that can be interpreted as the navigational performance of AUVs.

In this paper, we present an adaptive learning algorithm for controlled Lagrangian particle tracking. Previous work [8], [9] shows that CLPE can increase over time in simulated and field experiments because of inaccurate flow models included in the simulated motion models. Since CLPE represents the accuracy of the simulated motion models, the proposed algorithm employs learning models instead of the simulated models, and updates the learning models according to CLPE so that both the learning models and the vehicle motion model are identical.

Many researchers have developed path-planning algorithms to improve navigational performance of AUVs against complex ocean flows [10]–[12]. By assuming that the true flow field is well-represented by ocean models [13], [14], the path-planning algorithms generate reference trajectories through off-line computation on shore. Waypoints corresponding to the reference trajectories are commanded to the AUVs in the field.

However, "true" ocean flow fields are unknown, and ocean models can have significant error due to unknown or under-constrained boundary conditions, initial conditions, or missing physics [15], [16]. Thus, we cannot guarantee that true trajectories of AUVs are the same as the reference trajectories generated by path planning algorithms. Alternately, Lagrangian data assimilation schemes [4], [7], [17] and glider computerized tomography algorithms [18], [19] can be used to address the better identification of ocean flow using AUV-derived observations of the flow field. Such algorithms focus on updating flow models and mapping flows, and the algorithms can be complementary to our results.

For on-line learning models, we design two controllers, a motion controller and a learning controller. The first is designed for the motion of AUVs, and is composed of constant feedforward and feedback gains, plus a flow canceling term that uses a parametric flow model with known parameters. The second controller is designed to learn the motion of AUVs. In this learning controller, feedforward and feedback gains, learning parameters, and parameters of the flow canceling term are adapted by the proposed learning law based on CLPE. These controllers allow AUVs to learn their actual motion while identifying the ocean flow field.

We organize this paper into the following sections: Section II describes the problem setup introducing the vehicle mo-

978-1-5090-1537-5/16/$31.00 ©2016 IEEE

tion model, the learning model, flow models, and the state feedback controllers with flow canceling. Section III presents the adaptive learning algorithm, and analyzes robustness of the proposed algorithm. Section IV presents the simulation results that show the verification of the theoretical analysis, and Section V provides conclusions.

II. Problem Formulation

We present an adaptive learning algorithm using the framework of controlled Lagrangian particle tracking. To formulate the learning problem of AUVs influenced by the uncertain ocean flow, we describe the vehicle motion model, the learning model, flow models, and state feedback controllers.

A. Vehicle motion model

Let $D \subset \mathbb{R}^2$ be a domain. Then let $\mathbf{F}(\mathbf{x},t)$ be a deterministic ambient flow velocity, where $\mathbf{F}$:$D \times [0,\infty] \to \mathbb{R}^2$. Let $\mathbf{v}$ be a through-water velocity, or the controlled velocity of the AUV, where $\mathbf{v}$:$D \times [0,\infty] \to \mathbb{R}^2$.

$$\frac{d\mathbf{x}}{dt} = \mathbf{F}_R(\mathbf{x},t) + \mathbf{v}(\mathbf{x},t,\mathbf{z}_c(t)). \tag{1}$$

Subscript R for the flow $\mathbf{F}$ denotes a real ocean flow. $\mathbf{F}_R$ and $\mathbf{v}$ are locally Lipschitz in $\mathbf{x} = [x_1, x_2]^\top \in D$. $\mathbf{x}$ is the true position of the AUV. $\mathbf{z}_c(t) = [z_{1c}(t), z_{2c}(t)]^\top$ is the desired trajectory of the AUV.

B. Learning model

Learning models are used for generating the simulated positions of the vehicle. When we define $\mathbf{z}(t)$ as the simulated position of the vehicle from a learning model, the trajectory of the vehicle is generated by integrating the following learning model:

$$\frac{d\mathbf{z}}{dt} = \mathbf{F}_M(\mathbf{z},t) + \mathbf{v}(\mathbf{z},t,\mathbf{z}_c(t)), \tag{2}$$

where subscript M for the flow $\mathbf{F}$ is a modeled flow.

C. Flow models

Flow fields can be represented by spatial and temporal basis functions [20]. We consider that spatial and temporal basis functions are the combination of Gaussian radial and tidal basis functions, respectively. Let N be a positive integer, and θ, $\alpha_M \in \mathbb{R}^{2\times N}$. Let ϕ:$D \times [0,\infty] \to \mathbb{R}^N$ be $[\phi^1(\mathbf{x},t), \cdots \phi^N(\mathbf{x},t)]^\top$.

$$\begin{aligned} \mathbf{F}_R(\mathbf{x},t) &= \theta\phi(\mathbf{x},t) & (3)\\ \mathbf{F}_M(\mathbf{x},t) &= \alpha_M\phi(\mathbf{x},t), & (4) \end{aligned}$$

where

$$\theta = \begin{bmatrix}\theta_1\\ \theta_2\end{bmatrix} = \begin{bmatrix}\theta_1^1 & \cdots & \theta_1^N\\ \theta_2^1 & \cdots & \theta_2^N\end{bmatrix}, \alpha_M = \begin{bmatrix}\alpha_{M_1}\\ \alpha_{M_2}\end{bmatrix} = \begin{bmatrix}\alpha_{M_1}^1 & \cdots & \alpha_{M_1}^N\\ \alpha_{M_2}^1 & \cdots & \alpha_{M_2}^N\end{bmatrix}.$$

The combined basis functions are

$$\phi^i(\mathbf{x},t) = \exp^{-\frac{\|\mathbf{x}-\mathbf{c}_i\|}{2\sigma_i}} \cos(\omega_i t), \tag{5}$$

where $\mathbf{c}_i$ is the centers, σ_i is the widths, ω_i tidal frequencies, and $i = 1, \cdots, N$.

D. State feedback controllers with flow canceling

The flow canceling strategy is to cancel out flow velocity by controlling the heading angle of AUVs [9]. With the flow canceling strategy, we design two types of controllers as the combination of feedback and feedforward structures. Let $\alpha(t) = \begin{bmatrix}\alpha_1(t)\\ \alpha_2(t)\end{bmatrix} = \begin{bmatrix}\alpha_1^1(t) & \cdots & \alpha_1^N(t)\\ \alpha_2^1(t) & \cdots & \alpha_2^N(t)\end{bmatrix}$. Let $K_M(t) = \text{diag}\{K_{M_1}(t), K_{M_2}(t)\}$, and $\Gamma_M(t) = \text{diag}\{\Gamma_{M_1}(t), \Gamma_{M_2}(t)\}$ be diagonal matrices with time varying parameters. Let $K_D = \text{diag}\{K_{D_1}, K_{D_2}\}$, and $\Gamma_D = \text{diag}\{\Gamma_{D_1}, \Gamma_{D_2}\}$ be diagonal matrices with desired fixed parameters. Let $\Psi_L(t) \in \mathbb{R}^2$ is a learning injection parameter. Then,

$$\mathbf{v}(\mathbf{z},t,\mathbf{z}_c(t)) = -\alpha(t)\phi(\mathbf{z},t) - K_M(t)\mathbf{z} + \Gamma_M(t)\mathbf{z}_c(t) + \Psi_L(t) \tag{6}$$

$$\mathbf{v}(\mathbf{x},t,\mathbf{z}_c(t)) = -\alpha_M\phi(\mathbf{x},t) - K_D\mathbf{x} + \Gamma_D\mathbf{z}_c(t). \tag{7}$$

The learning controller represented by equation (6) contains (in order) a flow canceling term, a positional feedback term, a feedforward term, and a learning injection term with time varying parameters. By plugging equations (6) and (4) into equation (2), the closed loop dynamics under the learning controller is

$$\dot{\mathbf{z}} = (\alpha_M - \alpha(t))\,\phi(\mathbf{z},t) - K_M(t)\mathbf{z} + \Gamma_M(t)\mathbf{z}_c(t) + \Psi_L(t). \tag{8}$$

Meanwhile, the closed loop vehicle dynamics under the vehicle controller represented by equation (7) is

$$\dot{\mathbf{x}} = (\theta - \alpha_M)\phi(\mathbf{x},t) - K_D\mathbf{x} + \Gamma_D\mathbf{z}_c(t) \tag{9}$$

when we plug equations (7) and (3) into equation (1). If $\mathbf{x}$ and $\mathbf{z}$ have the same initial condition and $\alpha(t) = \alpha_M$, $K_M(t) = K_D$, $\Gamma_M(t) = \Gamma_D$, and $\Psi_L(t) = (\theta - \alpha_M)\phi(\mathbf{x},t)$, the learned trajectory is identical to the vehicle trajectory because of closed-loop dynamics. Our goal is to design the learning controller and the learning injection parameter so that the closed loop dynamics of the learning controller follows that of the vehicle controller.

E. Controlled Lagrangian prediction error

To develop the learning controller that makes the simulated trajectory follows the true trajectory in the ocean flow field, we first derive controlled Lagrangian prediction error (CLPE) dynamics that models how much the true trajectory is deviated from the simulated trajectory. By subtracting equation (8) from equation (9), CLPE dynamics is represented by

$$\begin{aligned} \dot{\mathbf{e}} &= \dot{\mathbf{x}} - \dot{\mathbf{z}}\\ &= (\theta - \alpha_M)\,\phi(\mathbf{x},t) - (\alpha_M - \alpha(t))\,\phi(\mathbf{z},t) - K_D\mathbf{x} + \Gamma_D\mathbf{z}_c(t)\\ &\quad + K_M(t)\mathbf{z} - \Gamma_M(t)\mathbf{z}_c(t) - \Psi_L(t)\\ &= (\theta - \alpha_M)\,\phi(\mathbf{x},t) - (\alpha_M - \alpha(t))\,\phi(\mathbf{z},t) + (K_M(t) - K_D)\,\mathbf{z}\\ &\quad - K_D\mathbf{e} + (\Gamma_D - \Gamma_M(t))\mathbf{z}_c(t) - \Psi_L(t). \end{aligned} \tag{10}$$

For example, if $\alpha(t) = \alpha_M$, $K_M(t) = K_D$, $\Gamma_M(t) = \Gamma_D$, and $\Psi_L(t) = (\theta - \alpha_M)\phi(\mathbf{x},t)$, CLPE goes to zero over time, which implies that the simulated trajectory follows the true trajectory. Our goal is to design a learning law for updating parameters

$\alpha(t)$, $K_M(t)$, and $\Gamma_M(t)$ by using CLPE dynamics so that CLPE converges to zero.

III. An adaptive learning algorithm

To design an adaptive learning algorithm for controlled Lagrangian particle tracking, we need some definitions and assumptions.

Definition 3.1 [21] Signal u is persistent exciting if there exist positive constants κ_1, κ_2, and T such that $\kappa_2 I > \int_t^{t+T} u(s)u^\top(s)ds > \kappa_1 I \ \forall t$.

Assumption 3.1 $\mathbf{z}_c$ is a persistent exciting signal.

Assumption 3.2 K_D, or the feedback gain matrix of equation (8), is positive definite.

Assumption 3.3 Let $\hat{\theta}$ be the estimate of θ. $\|\left(\theta-\hat{\theta}\right)\phi\|$ is bounded by flow velocity $f_{\max}$.

Remark 3.1 $\mathbf{z}_c$ is bounded because of persistent excitation.

Remark 3.2 Since θ is a unknown constant matrix, we can estimate θ using the Kalman filter and the motion tomography algorithm. We assume $\|\theta-\hat{\theta}\|$ can be bounded from those algorithms.

Remark 3.3 Positive definite matrix K_D is required for the vehicle controller with negative state feedback.

A. Using a flow model

This section addresses a learning controller that uses available modeled flows. We consider $\alpha(t)=\alpha_M$, which is available modeled flow. Then the CLPE dynamics from equation (10) becomes

$$\begin{aligned}\dot{\mathbf{e}} = &(\theta-\alpha_M)\,\phi(\mathbf{x},t) - K_D\mathbf{e} + (K_M(t)-K_D)\mathbf{z} \\ &+ (\Gamma_D-\Gamma_M(t))\mathbf{z}_c(t) - \Psi_L(t)\end{aligned} \tag{11}$$

Let $\bar{K}_M(t)=[K_{M_1}(t),\,K_{M_2}(t)]^\top$ and $\bar{\Gamma}_M=[\Gamma_{M_1}(t),\,\Gamma_{M_2}(t)]^\top$ be two dimensional vectors with time-varying parameters. Let $\bar{K}_D=[K_{D_1},\,K_{D_2}]^\top$, and $\bar{\Gamma}_D=[\Gamma_{D_1},\,\Gamma_{D_2}]^\top$ be two dimensional vectors with desired fixed parameters. Let $\tilde{\mathbf{z}}=\mathrm{diag}\{z_1,\,z_2\}$, and $\tilde{\mathbf{z}}_c=\mathrm{diag}\{z_{1c},\,z_{2c}\}$ be diagonal matrices. Let γ be any positive constant. We design learning parameter injection as follows:

$$\Psi_L(t)=(\theta-\alpha_M)\phi(\mathbf{x},t). \tag{12}$$

We have no knowledge of true flow parameter θ. When we use estimate $\hat{\theta}$ from known algorithms (e.g., Kalman filtering [17] or motion tomography [18]):

$$\Psi_L(t)=(\hat{\theta}-\alpha_M)\phi(\mathbf{x},t). \tag{13}$$

We design a learning law for time-varying parameters $\bar{K}_M$ and $\bar{\Gamma}_M$ by the following equations.

$$\dot{\bar{K}}_M(t) = -\gamma\tilde{\mathbf{z}}^\top\mathbf{e} \tag{14}$$

$$\dot{\bar{\Gamma}}_M(t) = \gamma\tilde{\mathbf{z}}_c^\top\mathbf{e} \tag{15}$$

Theorem 3.1 Under assumptions 3.1, 3.2, and 3.3, and using equations (13), (14), (15), CLPE is ultimately bounded by

$$\|\mathbf{e}\| \le \frac{1}{\mu}\|\left(\theta-\hat{\theta}\right)\phi(\mathbf{x},t)\| \tag{16}$$

where $\mu<\lambda_{\min}(K_D)$.

Proof. Consider a candidate Lyapunov function:

$$\begin{aligned}V(\mathbf{e},\bar{K}_M,\bar{\Gamma}_M) = \frac{1}{2}\Big\{&\mathbf{e}^\top\mathbf{e} + \frac{1}{\gamma}\left(\bar{K}_M-\bar{K}_D\right)^\top\left(\bar{K}_M-\bar{K}_D\right) \\ &+ \frac{1}{\gamma}\left(\bar{\Gamma}_D-\bar{\Gamma}_M\right)^\top\left(\bar{\Gamma}_D-\bar{\Gamma}_M\right)\Big\}.\end{aligned} \tag{17}$$

The derivative of V is

$$\begin{aligned}\dot{V} = &-\mathbf{e}^T K_D\mathbf{e} + \mathbf{e}^\top(\theta-\alpha_M)\,\phi(\mathbf{x},t) - \mathbf{e}^\top\Psi_L \\ &+ \left(\bar{K}_M-\bar{K}_D\right)^\top\left(\frac{1}{\gamma}\dot{\bar{K}}_M + \tilde{\mathbf{z}}\mathbf{e}\right) + \left(\bar{\Gamma}_D-\bar{\Gamma}_M\right)^\top\left(\tilde{\mathbf{z}}_c^\top\mathbf{e} - \frac{1}{\gamma}\dot{\bar{\Gamma}}_M\right).\end{aligned} \tag{18}$$

By assumption 3.2 and using equation (13), (14), and (15), $\dot{V} = -\mathbf{e}^\top K_D\mathbf{e} + \mathbf{e}^\top\left(\theta-\hat{\theta}\right)\phi(\mathbf{x},t)$. Then, $\dot{V} \le -\left(\lambda_{\min}(K_D)-\mu\right)\|\mathbf{e}\|^2 + \|\mathbf{e}\|\|\left(\theta-\hat{\theta}\right)\phi(\mathbf{x},t)\| - \mu\|\mathbf{e}\|^2$. When $\|\mathbf{e}\| \ge \frac{1}{\mu}\|\left(\theta-\hat{\theta}\right)\phi(\mathbf{x},t)\|$ given positive constant $\mu<\lambda_{\min}(K_D)$, $\dot{V} \le -\left(\lambda_{\min}(K_D)-\mu\right)\|\mathbf{e}\|^2$. This mean $\dot{V}$ is not positive. Thus, $\|\mathbf{e}\| \le \frac{1}{\mu}\|\left(\theta-\hat{\theta}\right)\phi(\mathbf{x},t)\|$. □

Remark 3.3 Theorem 3.1 shows that CLPE is bounded by estimated error of flow velocity as expected. Hence, the convergence of theorem 3.1 is completely determined by the accuracy of $\hat{\theta}$, which depends on the convergence of known algorithms (Kalman filtering, motion tomography [17], [18]). The following sections describes another learning algorithm that includes learning flows so that CLPE converges to zero.

B. Learning flow

We rewrite equation (10) as follows:

$$\begin{aligned}\dot{\mathbf{e}} = &(\theta+\alpha(t))\,\phi(\mathbf{x},t) + (K_M(t)-K_D)\,\mathbf{z} + (\Gamma_D-\Gamma_M(t))\mathbf{z}_c(t) \\ &- K_D\mathbf{e} - \Psi_L(t) - (\alpha_M+\alpha(t))\phi(\mathbf{x},t) - (\alpha_M-\alpha(t))\phi(\mathbf{z},t).\end{aligned} \tag{19}$$

Let $\bar{\theta}$, $\bar{\alpha}$, and $\overline{\mathbf{e}\phi^\top} \in \mathbb{R}^{2N}$ be row vectors. That is, $\bar{\alpha}(t) = [\alpha_1^1(t),\cdots,\alpha_1^N(t),\alpha_2^1(t),\cdots,\alpha_2^N(t)]$, $\bar{\theta}(t) = [\theta_1^1(t),\cdots,\theta_1^N(t),\theta_2^1(t),\cdots,\theta_2^N(t)]$, and $\overline{\mathbf{e}\phi^\top} = [e_1\phi_1,\cdots,e_1\phi_N,e_2\phi_1,\cdots,e_2\phi_N]^\top$. We design a learning parameter injection as follows:

$$\Psi_L(t) = -(\alpha_M+\alpha(t))\phi(\mathbf{x},t) - (\alpha_M-\alpha(t))\phi(\mathbf{z},t). \tag{20}$$

We design a learning law for time-varying parameters

$$\dot{\bar{\alpha}}(t) = -\gamma\overline{\mathbf{e}\phi^\top}(\mathbf{x},t) \tag{21}$$

$$\dot{\bar{K}}_M(t) = -\gamma\tilde{\mathbf{z}}^\top\mathbf{e} \tag{22}$$

$$\dot{\bar{\Gamma}}_M(t) = \gamma\tilde{\mathbf{z}}_c^\top\mathbf{e} \tag{23}$$

Theorem 3.2 Under assumptions 3.1 and 3.2, and using equations (20), (21), (22), and (23), CLPE converges to zero when time goes to infinity.

Proof. Consider a candidate Lyapunov function:

$$\begin{aligned}
&V(\mathbf{e},\alpha,\bar{K}_M,\bar{\Gamma}_M)\\
=&\frac{1}{2}\Big\{\mathbf{e}^\top\mathbf{e}+\frac{1}{\gamma}(\theta_1+\alpha_1(t))(\theta_1+\alpha_1(t))^\top\\
&+\frac{1}{\gamma}(\theta_2+\alpha_2(t))(\theta_2+\alpha_2(t))^\top+\frac{1}{\gamma}(\bar{K}_M-\bar{K}_D)^\top(\bar{K}_M-\bar{K}_D)\\
&+\frac{1}{\gamma}\left(\bar{\Gamma}_D-\bar{\Gamma}_M\right)^\top\left(\bar{\Gamma}_D-\bar{\Gamma}_M\right)\Big\}.
\end{aligned}\tag{24}$$

The derivative of V is

$$\begin{aligned}
\dot{V}=&-\mathbf{e}^T K_D\mathbf{e}+\mathbf{e}^\top(\theta+\alpha)\phi(\mathbf{x},t)-\mathbf{e}^\top\Psi_L-2\mathbf{e}^\top\alpha_M\phi(\mathbf{x},t)\\
&+(\bar{K}_M-\bar{K}_D)^\top\left(\frac{1}{\gamma}\dot{\bar{K}}_M+\tilde{\mathbf{z}}\mathbf{e}\right)+\left(\bar{\Gamma}_D-\bar{\Gamma}_M\right)^\top\left(\tilde{\mathbf{z}}_c^\top\mathbf{e}-\frac{1}{\gamma}\dot{\bar{\Gamma}}_M\right)\\
&+\frac{1}{\gamma}\left(\bar{\theta}+\bar{\alpha}\right)\dot{\bar{\alpha}}.
\end{aligned}\tag{25}$$

We know $\mathbf{e}^\top(\theta+\alpha)\phi=\left(\bar{\theta}+\bar{\alpha}\right)\overline{\mathbf{e}\phi^\top}$. Then, under assumption 3.2 and using equation (20), (21), (22), and (23),

$$\dot{V}=-\mathbf{e}^\top K_D\mathbf{e}\le 0.\tag{26}$$

$\dot{V}$ is negative semi-definite and this implies that $\mathbf{e}$, α, $\bar{K}_M$, and $\bar{\Gamma}_M$ are bounded. In addition, the second order time derivative of V satisfies $\ddot{V}=-2\mathbf{e}^\top K_D\dot{\mathbf{e}}=-2\mathbf{e}^\top K_D\{(\theta+\alpha)\phi(\mathbf{x},t)-K_D\mathbf{e}+(K_M(t)-K_D)\mathbf{z}+(\Gamma_D-\Gamma_M(t))\mathbf{z}_c-\Psi_L(t)-2\alpha_M\phi(\mathbf{x},t)\}$. From equation (20), Ψ_L is bounded. By assumption 3.1, $\mathbf{z}_c$ is bounded, and $\mathbf{z}$ is bounded because equation (8) represents linear systems with sinusoidal inputs. In addition, K_M, and Γ_M are bounded. Thus, $\ddot{V}$ is bounded, and hence $\dot{V}$ is uniformly continuous. By Barbalat's lemma in [22], [23], $\mathbf{e}\to 0$ when $t\to\infty$. □

Theorem 3.3 Under the same setting of theorem 3.2, $\bar{\alpha}$, $\bar{K}_M$, and $\bar{\Gamma}_M$ converges to $-\bar{\theta}$, $\bar{K}_D$, and $\bar{\Gamma}_D$, respectively.

Proof. In order to identify the ocean flow field from the proposed learning control law, we prove the convergence of parameters $\bar{\alpha}$, $\bar{K}_M$, and $\bar{\Gamma}_M$. Let η_1, η_2, η_3, and η_4 be $(\theta_1+\alpha_1)^\top$, $(\theta_2+\alpha_2)^\top$, $\bar{K}_M-\bar{K}_D$, and $\bar{\Gamma}_D-\bar{\Gamma}_M$, respectively. Let $\tilde{\phi}_1=\begin{bmatrix}\phi_1^1 & \cdots & \phi_1^N\\ 0 & \cdots & 0\end{bmatrix}$ and $\tilde{\phi}_2=\begin{bmatrix}0 & \cdots & 0\\ \phi_2^1 & \cdots & \phi_2^N\end{bmatrix}$ be in $\mathbb{R}^{2\times N}$. We rewrite equation (19) using equation η_1, η_2, η_3, and η_4 as follows:

$$\dot{\mathbf{e}}=\tilde{\phi}_1(\mathbf{x},t)\eta_1+\tilde{\phi}_2(\mathbf{x},t)\eta_2+\tilde{\mathbf{x}}\eta_3-K_D\mathbf{e}+\tilde{\mathbf{z}}_c\eta_4.\tag{27}$$

We augment $\mathbf{e}$, η_1, η_2, η_3, and η_4 to new state variable X. Then

$$\begin{aligned}
\dot{X}=A(t)X,\quad A(t)=&\begin{bmatrix}-K_D & \tilde{\phi}_1 & \tilde{\phi}_2 & \tilde{\mathbf{z}} & \tilde{\mathbf{z}}_c\\ -\gamma\tilde{\phi}_1 & 0 & 0 & 0 & 0\\ -\gamma\tilde{\phi}_2 & 0 & 0 & 0 & 0\\ -\gamma\tilde{\mathbf{z}} & 0 & 0 & 0 & 0\\ -\gamma\tilde{\mathbf{z}}_c & 0 & 0 & 0 & 0\end{bmatrix}\\
Y=CX,\quad C=&\begin{bmatrix}I & 0 & 0 & 0 & 0\\ 0 & 0 & 0 & 0 & 0\\ 0 & 0 & 0 & 0 & 0\\ 0 & 0 & 0 & 0 & 0\end{bmatrix}.
\end{aligned}\tag{28}$$

Our goal is to show the origin of $\dot{X}=A(t)X$ is uniformly asymptotically stable, which implies that $\bar{\alpha}=-\bar{\theta}$, $\bar{K}_M=\bar{K}_D$, and $\bar{\Gamma}_M=\bar{\Gamma}_D$. By theorem 3.4.8 in [24], a necessary and sufficient condition is that there exist a symmetric matrix P such that $c_1I\le P\le c_2I$ and $A^\top P+PA+\dot{P}+\nu C^\top C\le 0$ are satisfied $\forall t$ and some constant $\nu>0$, where $c_1>0$, and $c_2>0$ and C is such that (C,A) is a uniformly completely observable. Let $P=\begin{bmatrix}\frac{1}{2}K_D^{-1} & 0 & 0 & 0 & 0\\ 0 & \frac{1}{2\gamma}K_D^{-1} & 0 & 0 & 0\\ 0 & 0 & \frac{1}{2\gamma}K_D^{-1} & 0 & 0\\ 0 & 0 & 0 & \frac{1}{2\gamma}K_D^{-1} & 0\\ 0 & 0 & 0 & 0 & \frac{1}{2\gamma}K_D^{-1}\end{bmatrix}$. Let V' be $X^\top PX$. Then,

$$\dot{V}'=X^\top(A^\top P+P^\top A+\dot{P})X\le-\nu X^\top C^\top CX=-\nu\|Y\|^2,\tag{29}$$

where $\dot{P}=0$.

Now we will prove (C,A) is a uniformly completely observable. Because it is hard to prove the observability of time varying system matrix A, we will instead show $(C,A+LC)$ is uniformly completely observable with some bounded matrix L, called output injection by lemma 4.8.1 in [24]. Let $L=\begin{bmatrix}K_D & 0 & 0 & 0 & 0\\ \gamma\tilde{\phi}_1 & 0 & 0 & 0 & 0\\ \gamma\tilde{\phi}_2 & 0 & 0 & 0 & 0\\ \gamma\tilde{\mathbf{z}} & 0 & 0 & 0 & 0\\ \gamma\tilde{\mathbf{z}}_c & 0 & 0 & 0 & 0\end{bmatrix}$. Since $\mathbf{x}$ and $\mathbf{z}_c$ are bounded, and $\tilde{\phi}$ is a sinusoidal function with exponential magnitude, L is bounded. Then, A+LC = $\begin{bmatrix}0 & \tilde{\phi}_1 & \tilde{\phi}_2 & \tilde{\mathbf{z}} & \tilde{\mathbf{z}}_c\\ 0 & 0 & 0 & 0 & 0\\ 0 & 0 & 0 & 0 & 0\\ 0 & 0 & 0 & 0 & 0\\ 0 & 0 & 0 & 0 & 0\end{bmatrix}$. Thus,

$$\begin{aligned}
\dot{X}&=AX=(A+LC)X-LY\\
Y&=CX.
\end{aligned}\tag{30}$$

Let $\eta=[\eta_1,\ \eta_2,\ \eta_3,\ \eta_4]^\top$, and $w=[\tilde{\phi}_1,\ \tilde{\phi}_2,\ \tilde{\mathbf{z}},\ \tilde{\mathbf{z}}_c]^\top$. We have the following equation corresponding to equation (30).

$$\begin{aligned}
\dot{\mathbf{e}}&=-K_D\mathbf{e}+w^\top\eta\\
\dot{\eta}&=0\\
Y&=\mathbf{e}.
\end{aligned}\tag{31}$$

Because $\tilde{\mathbf{z}}_c$ is persistent exciting, $\tilde{\mathbf{z}}$ is bounded, and $\tilde{\phi}_1$ and $\tilde{\phi}_2$ are sinusoidal functions, w is persistent exciting. Let $\Phi(\zeta)=\int_t^\tau\exp^{-K_D(\tau-\zeta)}w(\zeta)d\zeta$. By lemma 4.8.3 in [24], $\Phi(\zeta)$ satisfies persistent exciting conditions because of a stable, minimum phase, proper rational transfer function $(sI_{2\times 2}+K_D)$. Therefore, there exists constant ρ_1, ρ_2, $T_0>0$ such that $\rho_2 I\ge\frac{1}{T_0}\int_t^{t+T_0}\Phi(\zeta)\Phi^\top(\zeta)d\zeta\ge\rho_1 I\ \forall t\ge 0$. By applying lemma 4.8.4 in [24] to the system of equation (31), $(C,A+LC)$ is uniformly completely observable; hence, the system of equation (28) is uniformly completely observable. Therefore, $\bar{\alpha}$, $\bar{K}_M$, and $\bar{\Gamma}_M$ converge to $-\bar{\theta}$, $\bar{K}_D$, and $\bar{\Gamma}_D$, respectively. □

C. Inaccuracy in flow modeling

Although the basis functions well capture the spatial variability of ocean flow in a specific region, the functions still include deterministic errors induced by the variability out of the region. In this section, we address the robustness of the proposed adaptive learning algorithms.

We show the boundedness of CLPE when the true flow model has unknown disturbances such as unstructured uncertainties. We assume $\mathbf{F}_R(\mathbf{x},t) = \theta\phi(\mathbf{x},t) + \Delta$, where $\|\Delta\|$ is bounded by $\Delta_{\max}$. Then,

$$\begin{aligned}\dot{\mathbf{e}} = &(\theta + \alpha(t))\,\phi(\mathbf{x},t) + (K_M(t) - K_D)\mathbf{z} - K_D\mathbf{e} \\ &+ (\Gamma_D - \Gamma_M(t))\mathbf{z}_c + \Delta.\end{aligned} \tag{32}$$

Theorem 3.4 Under the same setting of theorem 3.2, the bound of CLPE is

$$\|\mathbf{e}\| \leq \frac{1}{\beta}\|\Delta\| \tag{33}$$

where the positive constant $\beta < \lambda_{\min}(K_D)$.

Proof. Let V be the Lyapunov function represented by equation (24). By using equation (32), the derivate of V is

$$\begin{aligned}\dot{V} = &-\mathbf{e}^T K_D\mathbf{e} + \mathbf{e}^\top\Delta + (\bar{K}_M - \bar{K}_D)^\top\left(\frac{1}{\gamma}\dot{\bar{K}}_M + \tilde{\mathbf{z}}\mathbf{e}\right) \\ &+ \left(\bar{\Gamma}_D - \bar{\Gamma}_M\right)^\top\left(\tilde{\mathbf{z}}_c^\top\mathbf{e} - \frac{1}{\gamma}\dot{\bar{\Gamma}}_M\right) + \frac{1}{\gamma}\left(\bar{\theta} + \bar{\alpha}\right)\left(\frac{1}{\gamma}\dot{\bar{\alpha}} + \overline{\mathbf{e}\phi^\top}(\mathbf{x},t)\right)\end{aligned} \tag{34}$$

Then, we plug the adaptive law represented by equations (20), (21), (22), and (23) into equation (34). Then,

$$\begin{aligned}\dot{V} &= -\mathbf{e}^T K_D\mathbf{e} + \mathbf{e}^\top\Delta \\ &\leq -\lambda_{\min}(K_D)\mathbf{e}^\top\mathbf{e} + \mathbf{e}^\top\Delta \\ &\leq -\lambda_{\min}(K_D)\|\mathbf{e}\|^2 + \|\mathbf{e}\|\|\Delta\| \\ &\leq -\left(\lambda_{\min}(K_D) - \beta\right)\|\mathbf{e}\|^2 + \|\mathbf{e}\|\|\Delta\| - \beta\|\mathbf{e}\|^2\end{aligned} \tag{35}$$

When $\|\mathbf{e}\| \geq \frac{1}{\beta}\|\Delta\|$ given positive constant $\beta < \lambda_{\min}(K_D)$, $\dot{V} \leq -\left(\lambda_{\min}(K_D) - \beta\right)\|\mathbf{e}\|^2$, which means $\dot{V}$ is negative definite. Thus, CLPE is bounded by $\|\mathbf{e}\| \leq \frac{1}{\beta}\|\Delta\|$. □

IV. Simulation Results

In this section, we describe simulation results for the proposed learning algorithm. We choose 3 spatial and 3 tidal basis functions to represent 2D ocean flow along each of the two directions. θ_1, which represents true flow parameters along the horizontal direction, is [1.0 0.4 0.8]. θ_2, which represents three flow parameters along the vertical direction, is [0.9 0.4 0.8]. The three combined basis functions are represented by center c_i, width σ_i, and tidal frequency ω_i, where $i = 1,2,3$. c_1, c_2, and c_3 are $[0,0]^\top$, $[10,10]^\top$, and $[5,5]^\top$, respectively. σ_1, σ_2, and σ_3 are all equal to 5. We select three frequencies to represent tides, the M_2 lunar semidiurnal (period=12.42 hours), and two fictional frequencies with periods at intervals higher and lower than the M_2 (10.42, 24.42 hrs). Feedback gain of the vehicle controller, K_D is diag$\{1,1\}$. Γ_D is the same as K_D, and all parameters in the learning algorithm are initialized at 0. Adaptation speed, or γ is designed as 0.8. We consider 10 waypoints generated from $\mathbf{z}_c = [r\cos\Theta, r\sin\Theta]^\top$ with $r = 3$, and $\Theta = \frac{\pi}{5}\lfloor\frac{t}{20}\rfloor$. Figure 1 represents waypoints of the AUV. The AUV completes a cycle when it sequentially travels nine waypoints counter-clock direction from starting at waypoint (3,0), and arrives back at waypoint (3,0).

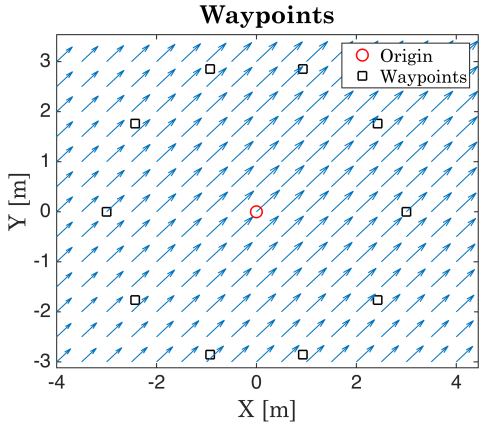

Fig. 1. An AUV starts to go to the waypoint (3,0) from the origin, and then keeps moving the next waypoint counter-clockwise direction. Arrows represents ocean flow at the initial time. Flow direction changes over time according to the tidal basis functions.

Figures 2, 3, 4 shows simulation results of CLPE and six flow parameters. CLPE goes to zero over 200 seconds (10 intervals), which is about one cycle. Moreover, the six flow parameters converges to their true flow parameters. Feedback and feedforward gains converge to the gains of desired controller with the similar trend of flow parameters. These results support our theoretical analysis in the previous section.

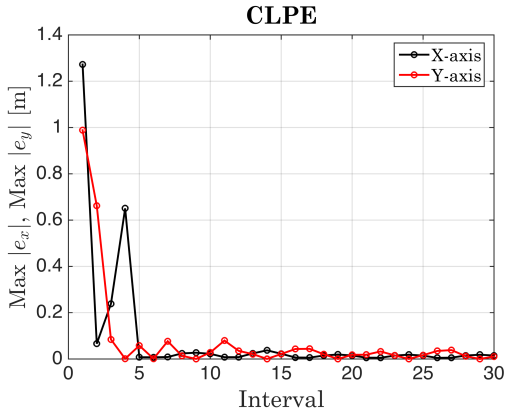

Fig. 2. CLPE: Each unit represents time interval of 20 seconds. 10 interval represents one cycle. Over one cycle, CLPE error is significantly reduced, and CLPE converges to zero.

V. Conclusion

We have developed an adaptive learning algorithm for controlled Lagrangian particle tracking (CLPT) that improves the ability of an AUV to sense the flow field in which its operates by incorporating the its navigation error. This improvement

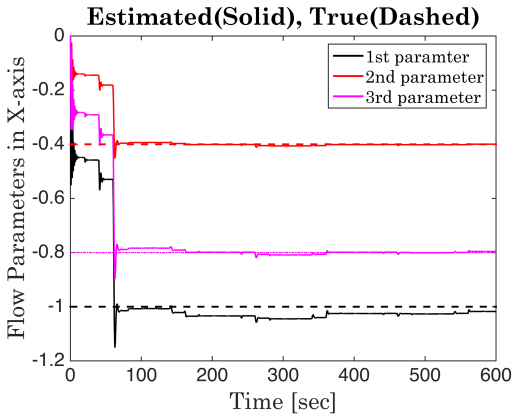

Fig. 3. Parameters for horizontal flow converges to true values.

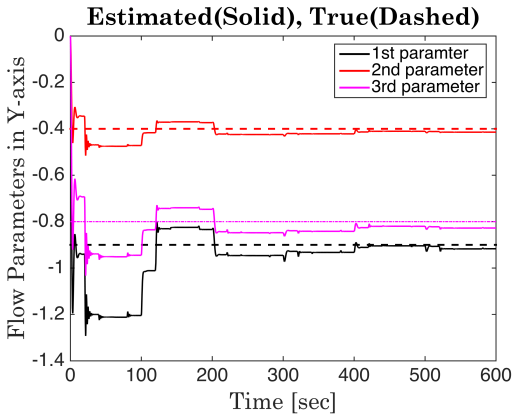

Fig. 4. Parameters for vertical flow converges to true values.

accelerates convergence in the estimation of flow as well as controller gains convergence to true gains. Furthermore, we prove that the algorithm guarantees controlled Lagrangian prediction error (CLPE) converges to zero with time. To address the robustness of the algorithm, we show that CLPE is ultimately bounded in terms of unknown disturbance in ocean flow.

No AUV is a perfect navigator; each is limited in its ability to navigate because of limits to propulsion mechanisms and self-localization. Future work will develop algorithms that address boundedness of the problem when the controlled velocity is saturated and develop learning algorithms when the localization service is infrequent.

ACKNOWLEDGMENTS

This research is supported by ONR grants N00014-14-1-0635, N00014-16-1-2667; NSF grants IIS-1319874, CMMI-1436284, CNS-0931576, OCE-1032285, OCE-1559475; and NOAA award NA16NOS0120028.

REFERENCES

[1] F. Zhang, G. Marani, R. N. Smith, and H. T. Choi, "Future trends in marine robotics," *IEEE Robotics and Automation Magazine*, vol. 22, no. 1, pp. 14–21, pp. 122, 2015.

[2] S. Mukhopadhyay, C. Wang, M. Patterson, M. Malisoff, and F. Zhang, "Collaborative autonomous surveys in marine environments affected by oil spills," *Cooperative Robots and Sensor Networks 2014*, vol. 554, pp. 87–113, 2014.

[3] W. Wu, A. Song, P. Varnell, and F. Zhang, "Cooperatively mapping of the underwater acoustic channel by robot swarms," in *Proceedings of the the Ninth ACM International Conference on Underwater Networks and Systems (WuWNet'14)*, 2014.

[4] N. E. Leonard, D. A. Paley, R. E. Davis, D. M. Fratantoni, F. Lekien, and F. Zhang, "Coordinated control of an underwater glider fleet in an adaptive ocean sampling field experiment in Monterey Bay," *Journal of Field Robotics*, vol. 27, no. 6, pp. 718–740, 2010.

[5] L. Paull, S. Saeedi, M. Seto, and H. Li, "Auv navigation and localization: A review," *IEEE Journal of Ocean Engineering*, vol. 39, no. 1, pp. 131–149, 2014.

[6] F. Zhang, D. M. Fratantoni, D. A. Paley, J. M. Lund, and N. E. Leonard, "Control of coordinated patterns for ocean sampling," *International Journal of Control*, vol. 80, no. 7, pp. 1186–1199, 2007.

[7] D. Chang, F. Zhang, and C. R. Edwards, "Real-time guidance of underwater gliders assisted by predictive ocean models," *Journal of Atmospheric and Oceanic Technology*, vol. 32, no. 3, pp. 562–578, 2015.

[8] K. Szwaykowska and F. Zhang, "Controlled Lagrangian particle tracking error under biased flow prediction," in *2013 American Control Conference*, Washington, DC, USA, 2013, pp. 2575–2580.

[9] ——, "Trend and bounds for error growth in controlled Lagrangian particle tracking," *IEEE Journal of Oceanic Engineering*, vol. 39, no. 1, pp. 10–25, 2014.

[10] B. Garau, M. Bonet, A. Alvarez, S. Ruiz, and A. Pascual, "Path planning for autonomous underwater vehicles in realistic oceanic current fields: Application to gliders in the western mediterranean sea," *Journal of Maritime Research*, vol. 6, no. 2, pp. 5–21, 2009.

[11] B. Rhoads, I. Mezic, and A. C. Poje, "Minimum time heading control of underpowered vehicles in time-varying ocean currents," *Ocean Engineering*, vol. 66, no. 1, pp. 12–31, 2012.

[12] A. A. Pereira, J. Binney, G. A. Hollinger, and G. S. Sukhatme, "Risk-aware path planning for autonomous underwater vehicles using predictive ocean models," *IEEE Journal of Field Robotics*, vol. 30, pp. 741–762, 2013.

[13] A. F. Shchepetkin and J. C. McWilliams, "The regional oceanic modeling system (ROMS): a split-explicit, free-surface, topography-following-coordinate oceanic model," *Ocean Modelling*, vol. 9, pp. 347–404, 2005.

[14] P. J. Martin, "Description of the navy coastal ocean model version 1.0," Naval Research Lab, Tech. Rep. NRL/FR/7322–00-9962, 2000.

[15] A. C. Haza, L. I. Piterbarg, P. Martin, T. M. Ozgokmen, and A. Griffa, "A Lagrangian subgridscale model for particle transport improvement and application in the Adriatic Sea using the Navy Coastal Ocean Model," *Ocean Modelling*, vol. 17, no. 1, pp. 68–91, 2007.

[16] A. Griffa, L. I. Piterbarg, and T. Ozgokmen, "Predictability of Lagrangian particle trajectories: Effects of smoothing of the underlying Eulerian flow," *Journal of Marine Research*, vol. 62, no. 1, pp. 1–35, 2004.

[17] D. Chang, X. Liang, W. Wu, C. R. Edwards, and F. Zhang, "Real-time modeling of ocean currents for navigating underwater glider sensing networks," *Cooperative Robots and Sensor Networks, Studies in Computational Intelligence*, vol. 507, pp. 61–75, 2014.

[18] W. Wu, D. Chang, and F. Zhang, "Glider CT: Reconstructing flow fields from predicted motion of underwater gliders," in *Proceedings of the Eighth ACM International Conference on Underwater Networks and Systems (WUWNet '13)*, no. 47, 2013.

[19] D. Chang, W. Wu, and F. Zhang, "Glider CT: Analysis and experimental validation," *Distributed Autonomous Robotic Systems*, vol. 112, pp. 285–298, November 2014.

[20] X. Liang, W. Wu, D. Chang, and F. Zhang, "Real-time modelling of tidal current for navigating underwater glider sensing networks," in *Procedia Computer Science*, vol. 10, 2012, pp. 1121–1126.

[21] H. K. Khalil, *Nonlinear Systems*, 2nd ed. Prentice Hall, 1996.

[22] K. J. Astrom and B. Wittenmark, *Adaptive Control*, 2nd ed. Addison-Wesley, 1995.

[23] H. K. Khalil, *Nonlinear Systems*, 3rd ed. Printice Hall, 2002.

[24] P. Ioannou and J. Sun, *Robust Adaptive Control*. Prentice Hall, 1996.